# Specific mode output from multimode fiber oscillators by designing rare earth doping profiles

Wang Wen-Liang(王文亮), Huang Liang-Jin(黄良金), Leng Jin-Yong(冷进勇)†,
Guo Shao-Feng(郭少锋), and Jiang Zong-Fu(姜宗福)

*College of Optoelectric Science and Engineering, National University of Defense Technology, Changsha* 410073, *China*

(Received 23 April 2014; revised manuscript received 5 May 2014; published online 16 July 2014)

Based on rate equations, a theoretical model of a fiber oscillator with a multimode gain fiber was built. We studied the effect of the rare earth doping profile in the core on the output characteristics of the multimode fiber oscillator. The results indicated that a pure fundamental mode can be obtained by partly doping the core of the large mode area (LMA) ytterbium doped fiber (YDF) in the fiber laser. Furthermore, a sole specific high-order mode can also be implemented by tailoring the rare earth doping profile according to the simulations. The mode coupling effect was also taken into account in the model. In spite of the mode coupling effect, the specific mode was able to dominate in the output of the fiber laser by utilizing the designed LMA YDF.

**Keywords:** fiber laser, rare earth doping profile, specific mode

**PACS:** 42.55.Wd, 42.81.Qb, 78.20.Ci **DOI:** 10.1088/1674-1056/23/9/094207

## 1. Introduction

In multimode fiber lasers or amplifiers, every supported transverse mode may be excited. In practice, many applications require high-power single-mode laser sources.[1–4] Mode selection techniques, such as coiling the fiber and tailoring the doping profiles, can be applied to generate the fundamental mode output. Hotoleanu *et al.*[5] have investigated the transverse mode discrimination in multimode fibers by spatially controlling the radial doping distribution; however, the behaviors of the transverse mode competition and the output power distribution of each mode were not discussed, although they were later studied by Gong *et al.*[6] Ye *et al.*[7] confined the Yb doping within a smaller radius in the center of the core of a few-mode large mode area (LMA) fiber. Consequently, the fundamental mode, which overlaps better with the Yb ions, obtains a higher gain than the higher order modes and dominates the output of an amplified spontaneous emission (ASE) source setup. Marciante *et al.*[8] demonstrated a confined-gain multimode fiber laser with a beam quality of 1.3 at all pumping levels. The majority of previous researchers have been interested in obtaining the fundamental mode output from fiber lasers. However, there are many fields that require a pure specific high-order mode. The relationship between the beam quality and the mode content in the fiber can then be investigated conveniently. The mode dependent absorption or coupling of the fiber components can also be studied. Quimby *et al.*[9] employed a gain fiber with the ring doping position coincided with the $LP_{07}$ mode intensity distribution to suppress the ASE in high-power 977 nm lasers and amplifiers. The goal of this paper is to discuss how to obtain a single specific order mode by spatially controlling the radial doping distribution in a multimode active fiber, paying attention to the mode coupling effect on the transverse mode competition in the fiber laser.

## 2. Theoretical model

The model of an end-pumped fiber laser, which normally employs a typical linear cavity[10], is schematically illustrated in Fig. 1. The length of the gain double clad fiber (DCF) is $L$.

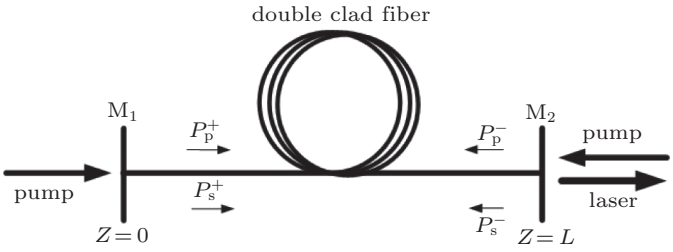



**Fig. 1.** Schematic illustration of the end-pumped fiber laser.

We assume that the pump light is homogeneous over the cross section of the fiber cladding, the ASE is ignored, and only one single longitudinal mode exists in the fiber laser. Based on the rate equations presented in Ref. [6], the model to describe the transverse mode competition in multimode fiber lasers can be expressed by the following equations:

$$\pm\frac{\mathrm{d}P_{si}^{\pm}(z)}{\mathrm{d}z}=\left\{\int_0^{2\pi}\int_0^{a}[(\sigma_{\mathrm{as}}+\sigma_{\mathrm{es}})N_2(r,\varphi,z)-\sigma_{\mathrm{as}}N(r,\varphi,z)]\Gamma_{si}(r,\varphi)r\,\mathrm{d}r\,\mathrm{d}\varphi\right\}P_{si}^{\pm}(z)-\alpha_{si}P_{si}^{\pm}(z)$$

†Corresponding author. E-mail: lengjy@sina.com

© 2014 Chinese Physical Society and IOP Publishing Ltd 

$$-\sum_j d_{ij}[P_{si}^{\pm}(z)-P_{sj}^{\pm}(z)], \tag{1}$$

$$\pm\frac{\mathrm{d}P_{\mathrm{p}}^{\pm}(z)}{\mathrm{d}z}=\left\{\int_0^{2\pi}\int_0^{a}[(\sigma_{\mathrm{ap}}+\sigma_{\mathrm{ep}})N_2(r,\varphi,z)-\sigma_{\mathrm{ap}}N(r,\varphi,z)]\Gamma_{\mathrm{p}}(r,\varphi)r\,\mathrm{d}r\,\mathrm{d}\varphi\right\}P_{\mathrm{p}}^{\pm}(z)-\alpha_{\mathrm{p}}P_{\mathrm{p}}^{\pm}(z), \tag{2}$$

$$\frac{N_2(r,\varphi,z)}{N(r,\varphi,z)}=\frac{\dfrac{[P_{\mathrm{p}}^{+}(z)+P_{\mathrm{p}}^{-}(z)]\sigma_{\mathrm{ap}}\Gamma_{\mathrm{p}}(r,\varphi)\lambda_{\mathrm{p}}}{hc}+\sum_i\dfrac{[P_{si}^{+}(z)+P_{si}^{-}(z)]\sigma_{\mathrm{as}}\Gamma_{si}(r,\varphi)\lambda_{\mathrm{s}}}{hc}}{\dfrac{[P_{\mathrm{p}}^{+}(z)+P_{\mathrm{p}}^{-}(z)](\sigma_{\mathrm{ap}}+\sigma_{\mathrm{ep}})\Gamma_{\mathrm{p}}(r,\varphi)\lambda_{\mathrm{p}}}{hc}+\dfrac{1}{\tau}+\sum_i\dfrac{[P_{si}^{+}(z)+P_{si}^{-}(z)](\sigma_{\mathrm{as}}+\sigma_{\mathrm{es}})\Gamma_{si}(r,\varphi)\lambda_{\mathrm{s}}}{hc}}, \tag{3}$$

where $P_{si}^{+}$ and $P_{si}^{-}$ are the signal powers of the $i$-th transverse mode in the forward and the backward directions, respectively; $P_{\mathrm{p}}^{+}$ and $P_{\mathrm{p}}^{-}$ are the pump powers in the forward and the backward directions, respectively; $N_2$ is the $Yb^{3+}$ concentration of the upper level; and, $N$ is the $Yb^{3+}$ concentration in the fiber. The variables $\Gamma_{\mathrm{p}}$ and $\Gamma_{si}$ stand for the power fill factors of the pump and the signal in the fiber laser; $\Gamma_{\mathrm{p}}$ is the core to inner cladding area ratio; while $\Gamma_{si}$ can be obtained by the mode theory of optical fiber. The variables $\sigma_{\mathrm{a(e)p}}$ and $\sigma_{\mathrm{a(e)s}}$ represent the absorption and the emission cross-sections of the pump and the signal, respectively. The $h$ is Planck's constant, and $c$ is the speed of light in vacuum. Here, $\alpha_{\mathrm{p}}$ and $\alpha_{si}$ represent the scattering loss coefficients of the pump and the signal, respectively; $\tau$ is the spontaneous radiative lifetime; $\lambda_{\mathrm{p}}$ and $\lambda_{\mathrm{s}}$ represent the wavelengths of the pump and the signal, respectively; and, $d_{ij}$ is the mode coupling coefficient between the $i$-th and the $j$-th transverse modes.

In this model, the reflection indices of the cavity mirrors for each transverse mode of the signal light are assumed to be the same, and then the cavity mirrors do not have a mode distinguishable effect. The boundary conditions of the fiber lasers are given by[6]

$$\begin{cases}P_{si}^{+}(0)=R_1P_{si}^{-}(0),\\ P_{si}^{-}(L)=R_2P_{si}^{+}(L),\end{cases} \tag{4}$$

where $L$ is the fiber length; and, variables $R_1$ and $R_2$ represent the reflection ratios of the cavity mirrors $M_1$ and $M_2$ at the signal wavelength, respectively.

Equations (1) and (2) describe the evolution of the pump and the signal along the fiber length. The cross mode coupling is taken into account, which will result in mode conversion and also affect the output intensity distribution. The overlap between the gain doping profile and the mode distribution, which also plays a decisive role in the output mode of the fiber laser, can be expressed as

$$\Gamma=\frac{\iint\Psi_1(x,y)\Psi_2(x,y)\,\mathrm{d}x\mathrm{d}y}{\sqrt{\iint\Psi_1^2(x,y)\,\mathrm{d}x\mathrm{d}y\iint\Psi_2^2(x,y)\,\mathrm{d}x\mathrm{d}y}}, \tag{5}$$

where $\Psi_1(x,y)$ and $\Psi_2(x,y)$ are the gain doping profile and one specific mode distribution, respectively. In this paper, we design the gain doping profile to achieve a specific mode output from the fiber laser.

## 3. Numerical simulation and result analysis

### 3.1. Parameters

The step refractive index distribution of a Yb doped DCF is discussed in this section. The fiber laser parameters are listed in Table 1.

**Table 1.** Parameters used in the simulation.

| Parameter | Value | Parameter | Value |
|---|---|---|---|
| Core diameter | 28 μm | Pump attenuation coefficient $\alpha_{\mathrm{p}}$ | $2\times10^{-3}$ m$^{-1}$ |
| Inner-clad diameter | 500 μm | Signal attenuation coefficient $\alpha_{\mathrm{s}}$ | $4\times10^{-4}$ m$^{-1}$ |
| NA of the core | 0.06 | Spontaneous lifetime $\tau$ | $0.8\times10^{-3}$ s |
| NA of the inner-clad | 0.46 | Reflection of $M_1$ at signal light $R_1$ | 1 |
| Refraction index of the core $n_{\mathrm{core}}$ | 1.459 | Reflection of $M_2$ at signal light $R_2$ | 0.04 |
| Refraction index of the inner-clad $n_{\mathrm{clad}}$ | 1.4577 | Reflection of $M_1$ at pump light | 0 |
| Pump center wavelength $\lambda_{\mathrm{p}}$ | 976 nm | Reflection of $M_2$ at pump light | 0 |
| Signal center wavelength $\lambda_{\mathrm{s}}$ | 1070 nm | Density of Yb | $4.6\times10^{25}$ m$^{-3}$ |

According to the parameters of the optical fiber, four transverse modes can be excited in the core, namely: $LP_{01}$, $LP_{11}$, $LP_{21}$, and $LP_{02}$. Assuming the usual Bessel function solution for the step-index fiber, we find the intensity distributions as shown in Fig. 2. It should be pointed out that, for the $LP_{mn}$ mode, those modes with $m\neq0$ must be considered twice for having two helical polarities. In Figs. 2(b) and 2(c), only one spatial pattern for $LP_{11}$ and $LP_{21}$ is presented.

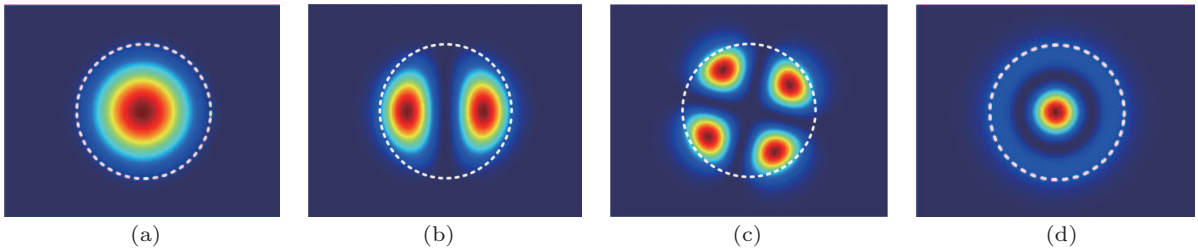



**Fig. 2.** (color online) Mode field distributions of (a) $LP_{01}$; (b) $LP_{11}$; (c) $LP_{21}$; and (d) $LP_{02}$.

The output characteristics of the fiber laser with various doping profiles will be discussed using the multilayer method.[6] The cross section of the fiber core is divided into a finite number of distinctive layers, each of which is so thin that the doping concentration and the population inversion can be regarded as constants in one layer. The number of the divided layers is 100 in our stimulation.

### 3.2. Fundamental mode output

In order to obtain a pure fundamental mode in a fiber oscillator, three kinds of doping distributions are considered, as shown in Fig. 3, where $N$ is the density of $Yb^{3+}$, $\rho$ denotes the normalized radius corresponding to the core radius, and $N(\rho)$ is the $Yb^{3+}$ concentration at position $\rho$. We discuss these specially doped gain fibers in a fiber oscillator, instead of the more complicated fiber amplifier that was discussed in Ref. [9].

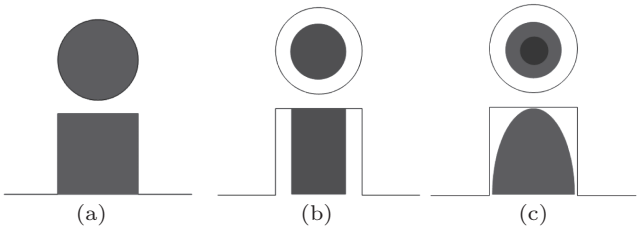



**Fig. 3.** (color online) Various doping profiles: (a) $N(\rho) = \begin{cases} N, & (\rho \le 1), \\ 0, & (\rho > 1), \end{cases}$ (b) $N(\rho) = \begin{cases} N, & (\rho \le 0.75), \\ 0, & (\rho > 0.75), \end{cases}$ and (c) $N(\rho) = \begin{cases} N, (1-\rho^2), & (\rho \le 1), \\ 0, & (\rho > 1). \end{cases}$

Firstly, we assume that the doped fiber is perfect without any defect and is not subject to any outside interference, so the coupling effect between the modes is ignored; that is, $d_{ij} = 0$ in Eq. (1).

The forward end-pumping scheme is analyzed. And the pump power is set to 50 W. The DCF with the various doping distributions acts as the gain medium. Based on the above mentioned model of the DC fiber laser, and by using the forth-order Runge–Kutta method, the pump and the signal power distributions along the fiber length in the oscillator are found, as shown in Fig. 4.

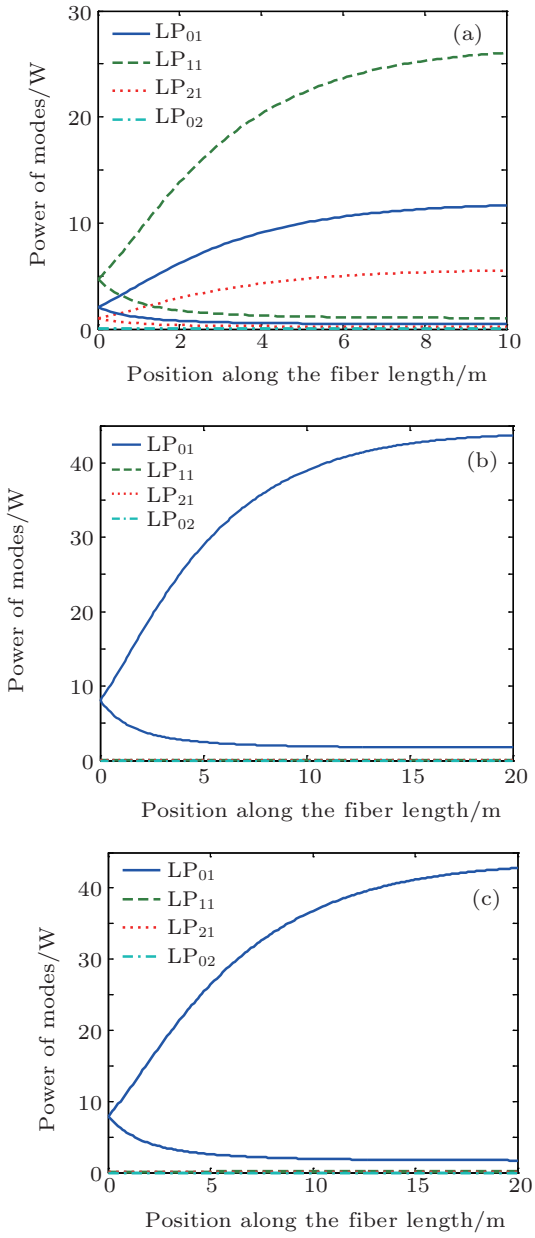



**Fig. 4.** (color online) Power evolution of each mode in the fiber lasers with various doping profiles, panels (a)–(c) correspond to the doping profiles shown in Figs. 3(a)–3(c), respectively.

The output characteristics, such as the optimum length of the oscillator, the output power, and the power percentage of each mode, are shown in Table 2. The output power is the maximum power in each case, with the optimum fiber length.

**Table 2.** Characteristics of the fiber lasers with various doping profiles in Fig. 3 in the absence of the coupling effect.

| Doping profile | Fiber length/m | Output power/W | Percentage of $LP_{01}$/% | Percentage of $LP_{11}$/% | Percentage of $LP_{21}$/% | Percentage of $LP_{02}$/% |
|---|---|---|---|---|---|---|
| Fig. 3(a) | 10 | 41.1 | 26.9 | 60.1 | 12.8 | 0.2 |
| Fig. 3(b) | 20 | 41.9 | 100 | 0 | 0 | 0 |
| Fig. 3(c) | 20 | 41.3 | 99.5 | 0.5 | 0 | 0 |

The results show that the optimum fiber length is shorter when the doped area is larger. The optimum fiber length of case (a) is the shortest. This is obvious and it can be attributed to the higher number of doping ions per meter. In addition, the output characteristics of the multimode fiber laser are affected by the rare earth doping profile. In case (a), all modes except $LP_{02}$ are excited and $LP_{11}$ is dominant among the four modes, which is not beneficial to the fundamental mode operation. In cases (b) and (c), the fundamental mode $LP_{01}$ dominates in the output and the high-order modes are suppressed to bleach the gain in the un-doped region. The doping profile in case (c) is more complicated and unfeasible compared to that in case (b).

In practice, the coupling effect between the adjacent modes is unavoidable and must be taken into consideration. The mode coupling in the multimode fiber is very complex, which may be caused by many factors,[6] including the internal flaw generated during the fabrication of the fiber and other external disturbances such as bending and twisting. Consequently, it is difficult to determine the mode coupling coefficient $d_{ij}$ in experiments. The mode coupling effect between the adjacent modes is much stronger than that between the nonadjacent modes.[11–14] Therefore, we assume that the coupling coefficient between the adjacent modes is 0.001 $m^{-1}$ (the value is from Ref. [6]), and that between the nonadjacent modes is zero. The adopted coupling coefficient can be used when the fiber is less-flawed or when the bending radius of the gain fiber is large enough. In this case, the output characteristic of each oscillator with various doping distributions are recalculated and shown in Table 3. This is more in agreement with the actual situation if the mode coupling is considered.

**Table 3.** Characteristics of the fiber lasers with various doping profiles in Fig. 3 in the presence of the coupling effect.

| Doping profile | Fiber length/m | Output power/W | Percentage of $LP_{01}$/% | Percentage of $LP_{11}$/% | Percentage of $LP_{21}$/% | Percentage of $LP_{02}$/% |
|---|---|---|---|---|---|---|
| Fig. 3(a) | 10 | 41.6 | 28.4 | 48.6 | 20.3 | 2.7 |
| Fig. 3(b) | 15 | 42.0 | 90.4 | 9.3 | 0.3 | 0 |
| Fig. 3(c) | 20 | 41.4 | 84.5 | 14.6 | 0.9 | 0 |

As shown in Table 3, the coupling effect between the modes strongly affects the output mode power distribution, and the effect is much more apparent in case (c) than that in cases (a) and (b). In case (b), the $LP_{01}$ mode dominates, even with the mode coupling effect. Furthermore, the above three cases are all sensitive to the mode coupling effect, even through the coupling effect between the adjacent modes is slight. By taking the optimum fiber length, the sensitivity of the mode coupling effect, and the complexity of the special doped fiber fabrication procedure into account, we find that case (b) is the best choice to achieve the fundamental mode output in the high power fiber oscillator with a multimode gain fiber. Note that, by carefully designing the doping percentage of case (b), we can achieve an even better result. The theoretical result is in agreement with the experimental results in Ref. [8].

### 3.3. Sole specific high-order mode output

In order to obtain only one given high-order mode output in a fiber laser, four ring doped profiles are designed, as shown in Fig. 5.

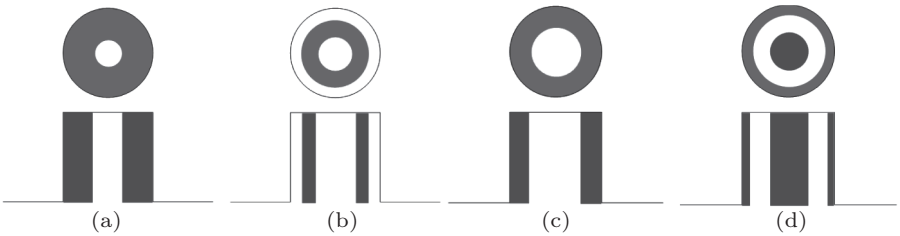



**Fig. 5.** (color online) Various doping profiles for specific high-order mode output: (a) $N(\rho) = \begin{cases} 0, & (\rho < 2), \\ N, & (0.2 \le \rho \le 1), \\ 0, & (\rho > 1), \end{cases}$ (b) $N(\rho) = \begin{cases} 0, & (\rho < 0.5), \\ N, & (0.5 \le \rho \le 0.7), \\ 0, & (\rho > 0.7), \end{cases}$ (c) $N(\rho) = \begin{cases} 0, & (\rho < 0.6), \\ N, & (0.6 \le \rho \le 1), \\ 0, & (\rho > 1), \end{cases}$ and (d) $N(\rho) = \begin{cases} N, & (\rho < 0.43), \\ 0, & (0.43 \le \rho \le 0.86), \\ N, & (0.86 \le \rho \le 1), \\ 0, & (\rho > 1). \end{cases}$

The mode coupling effect between the modes is also provisionally ignored. All of the parameters and conditions are the same as those in Subsection 3.2. Figure 6 shows the pump and the signal power distributions along the fiber length in the oscillator.

Characteristics such as the optimum length of the oscillator, the output power, and the power percentage of each mode, are calculated and shown in Table 4. Interestingly, the results indicate that the specific high-order modes can be achieved by designing the gain doped profiles. In cases (a) and (b), the first high order mode $LP_{11}$ is the dominant mode in the output, while $LP_{21}$ and $LP_{02}$ are the main modes in cases (c) and (d), respectively. The results are achieved under the ideal condition in the absence of the mode coupling effect.

The coupling effect between the adjacent modes is then taken into consideration. It is still supposed that $d_{ij} = 0.001$ for the adjacent modes and $d_{ij} = 0$ for the nonadjacent modes. The results are given in Table 5.

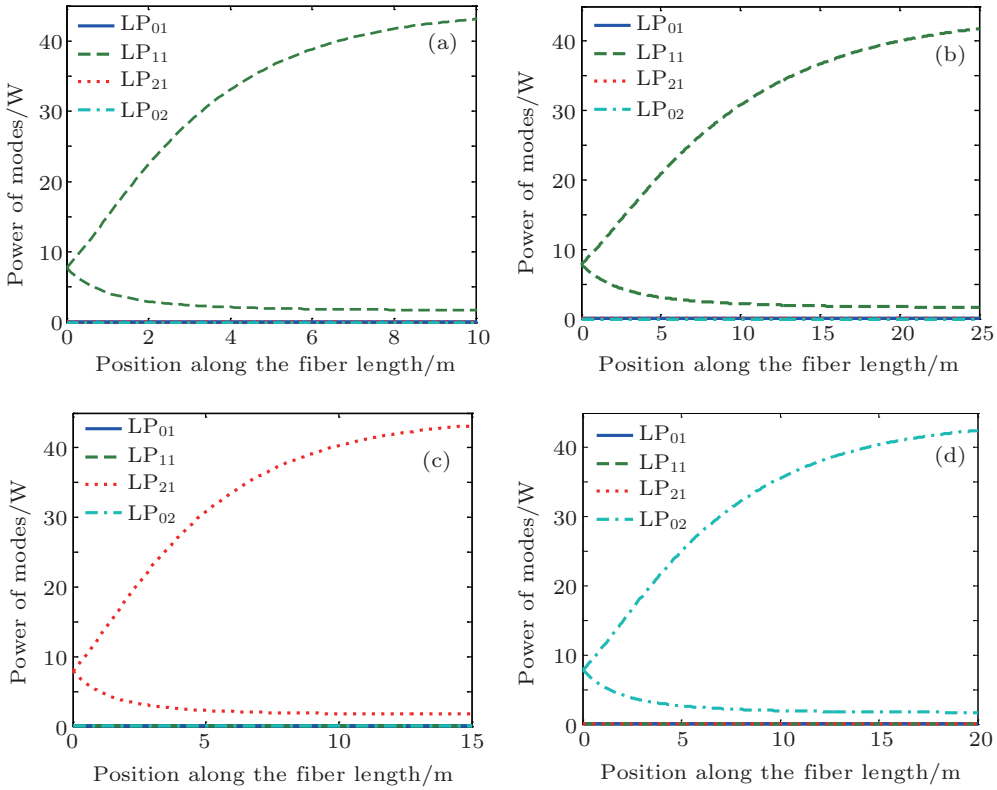



**Fig. 6.** (color online) Power evolution of each mode in the fiber lasers with various doping profiles, panels (a)–(d) correspond to the doping profiles shown in Figs. 5(a)–5(d), respectively.

**Table 4.** Characteristics of the fiber lasers with various doping profiles in Fig. 5 without the coupling effect.

| Doping profile | Fiber length/m | Output power/W | Percentage of $LP_{01}$/% | Percentage of $LP_{11}$/% | Percentage of $LP_{21}$/% | Percentage of $LP_{02}$/% |
|---|---|---|---|---|---|---|
| Fig. 5(a) | 10 | 41.7 | 0 | 100 | 0 | 0 |
| Fig. 5(b) | 25 | 40.1 | 0 | 100 | 0 | 0 |
| Fig. 5(c) | 15 | 41.5 | 0 | 0 | 100 | 0 |
| Fig. 5(d) | 20 | 40.8 | 0 | 0 | 0 | 100 |

**Table 5.** Characteristics of the fiber lasers with various doping profiles listed in Fig. 5 with the coupling effect.

| Doping profile | Fiber length/m | Output power/W | Percentage of $LP_{01}$/% | Percentage of $LP_{11}$/% | Percentage of $LP_{21}$/% | Percentage of $LP_{02}$/% |
|---|---|---|---|---|---|---|
| Fig. 5(a) | 10 | 41.4 | 11.1 | 72.9 | 15.4 | 0.6 |
| Fig. 5(b) | 25 | 40.1 | 7.2 | 85.1 | 7.5 | 0.2 |
| Fig. 5(c) | 15 | 41.4 | 0.1 | 5.7 | 91.9 | 2.3 |
| Fig. 5(d) | 20 | 40.8 | 0 | 0.2 | 4.5 | 95.3 |

The output characteristics in case (a) are more sensitive to the mode coupling effect than those in case (b). The power percentage of the $LP_{11}$ mode decreases due to the mode coupling effect but is still more than 85% in case (b). In case (c), the power percentage of the $LP_{21}$ mode is more than 90%, in spite of the mode coupling effect. In addition, case (d) has the benefit of $LP_{02}$ mode emission. In this case, the output characteristics are not subject to the mode coupling effect and the effect only reduces about 5% of the $LP_{21}$ mode.

Comparing the mode fields with the doping profiles, we can see that, when the doping position coincides with the sole mode intensity distribution, the matched mode obtains almost all gain while the other modes obtain little gain. In order to obtain a unique specific mode, such as $LP_{01}$, $LP_{11}$, $LP_{21}$, and $LP_{02}$, the doping profile of the gain fiber can be designed as above. Note that these designed LMA ytterbium doped fibers can be fabricated by the modified chemical vapor deposition method. Based on the simulations, the output mode of the fiber oscillator can be effectively controlled by spatially designing the gain doping distribution of the DCF. Eventually, we can obtain a single specific mode by using this method.

## 4. Conclusion

We have analyzed the influence of the gain doping distribution on the characteristics of a fiber oscillator in detail. The results indicate that a sole specific mode laser output, not only the fundamental mode but also the higher-order mode, can be obtained by designing the rare earth doping distribution of the LMA DCF, even considering the mode coupling effect. These theoretical research results are significant to the practical research of the design and mode control of fiber oscillators.

## References


[1] Richardson D J, Nilsson J and Clarkson W A 2010 *J. Opt. Soc. Am. B* **27** B63

[2] Chen Y E, Wang Y and Qu X L 2012 *Chin. Phys. Lett.* **29** 074214

[3] Zhou P, Wang X L, Ma Y X, Ma H T, Xu X J and Liu Z J 2009 *Chin. Phys. Lett.* **26** 084205

[4] Hao J P, Yan P, Xiao Q R, Li D and Gong M L 2014 *Chin. Phys. B* **23** 014204

[5] Hotoleanu M, Derlund M and Kliner D 2006 *Proceedings of SPIE Photonics West* **2006** 610264

[6] Gong M, Yuan Y, Li C, Yan P, Zhang H and Liao S 2007 *Opt. Express* **15** 3236

[7] Ye C, Koponen J, Kokki T, Ponsoda J M, Tervonen A and Honkanen S 2012 *Proceedings of the SPIE* **8237** 823737

[8] Marciante J R, Roides R G, Shkunov V V and Rockwell D A 2010 *Opt. Lett.* **35** 1828

[9] Quimby R S, Morse T F, Shubochkin R L and Ramachandran S 2009 *IEEE J. Quantum Electron* **15** 12

[10] Zhang C S, Zhang Q and Li L J 2004 *Acta Phys. Sin.* **53** 4262 (in Chinese)

[11] Kang Q, Lim E Lg, Jung Y, Sahu J K, Poletti F, Baskiotis C, Alam S and Richardson D J 2012 *Opt. Express* **20** 835

[12] Marcuse D 1974 *Theory of Dielectric Optical Waveguides* (2nd edn.) (London: Academic Press) p. 100

[13] Wang X, Xiong C and Luo J 2009 *Opt. Commun.* **282** 382

[14] Snyder A W and Love J D 1983 *Optical Waveguide Theory* (1st edn.) (New York: Chapman and Hall) pp. 509–535